



## Research article

Holistic approach to microwave-reflux extraction and thermo-analytical fingerprints of under-utilized *Artocarpus heterophyllus* seed wastesOlusegun Abayomi Olalere<sup>a,\*</sup>, Chee-Yuen Gan<sup>a,\*\*</sup>, Hamid Nour Abdurahman<sup>b</sup>, Oladayo Adeyi<sup>c</sup>, Mani Malam Ahmad<sup>d</sup><sup>a</sup> Analytical Biochemistry Research Centre (ABrC), Universiti Sains Malaysia (USM), 11800, Gelugor, Penang, Malaysia<sup>b</sup> Department of Chemical Engineering, Universiti Malaysia Pahang, 26300, Gambang, Malaysia<sup>c</sup> Department of Chemical Engineering, Michael Okpara University of Agriculture, Umudike, Nigeria<sup>d</sup> Department of Biological Science, Kano University of Science and Technology, Kano, Nigeria

## ARTICLE INFO

## Keywords:

Food science  
Organic product chemistry  
*Artocarpus heterophyllus*  
Bioactive  
Microwave-assisted extraction  
Spectrometry  
Taguchi method

## ABSTRACT

The increase in wastes generated from jackfruit seeds has been largely under-utilized in Malaysia. Due to the high nutritional and medicinal content embedded in the cellulosic structure of jackfruit wastes, a need then arises for their physicochemical elucidations. In this study, the extraction of *Artocarpus heterophyllus* seed was carefully investigated using Taguchi orthogonal optimization design. Complete functional group characteristics and chemical profile of the *A. heterophyllus* seed extracts were obtained using different physicochemical characterization. The optimal conditions of the microwave extraction parameters were determined at 5 min of irradiation time, 450 W of power and 50 °C of temperature. Under this condition, the optimal yield of 17.34 (mg/g) % was achieved at an SNR ratio of 24.78. The mass spectrometry analysis tentatively identified a total of 90 and 148 secondary metabolites at positive and negative ESI modes, respectively. The chemical profile obtained provided a baseline reference for further investigation on the food and medicinal bioactive from *Artocarpus heterophyllus* seed oleoresins. The FT-infrared emission spectrum shows the presence of some specific carbohydrates and amide protein functional groups directly linked to C–O (1008 cm<sup>-1</sup>) the carbonyl (C=O) groups, respectively. Moreover, the morphological characteristics of the jackfruit raw and crude extracts conspicuously revealed large-sized globules which suggest the carbohydrates and protein contents. The result of this study indicates that the use of microwave extraction technology produced high-quality extracts with lower degradation of the thermal labile constituents. This will assist in determining the suitable conditions necessary for the total recovery of medicinal and nutritional constituents and conversion of agricultural waste products into useful products.

## 1. Introduction

Jackfruit (*Artocarpus heterophyllus*) is an important fruit-bearing tree, grown in many parts of India, Myanmar, Sri-Lanka, Indonesia, and Malaysia (Balamaze et al., 2019). It is commonly regarded as the world largest tree-born fruit, ranked after mango and banana (Rana-singhe et al., 2019). The epidemiological investigation of this commodity plant has exposed its phytochemical richness which largely attests to its functional health benefits for the treatment of many life-threatening diseases (Balamaze et al., 2019). However, the large tonnes of jackfruit seeds wastes generated are mostly under-utilized with their accumulation posing a deleterious threat to the

environment, hence raising the need for their alternative environmentally-friendly applications (Jiang et al., 2019). Zhang et al. (2018) reported starch and proteins as the major components of jackfruits seeds. The jackfruit seeds contain 63% crude starch, 8% crude protein, 1.5 % crude fat and 2.2% ash content when taken on a dry basis (Zhang et al., 2016). Their high starch and protein content accounts for the shorter shelf life of their seeds most especially when temperature and humidity are high (Zhang et al., 2019). Hence in preserving the seeds, a lower temperature and humidity must be maintained most especially for experimental purposes. Moreover, since Jackfruit seed wastes' constituents are mainly starch and protein, there is need to select environmentally friendly solvents which will

\* Corresponding author.

\*\* Corresponding author.

E-mail addresses: [olabayor@usm.my](mailto:olabayor@usm.my) (O.A. Olalere), [cygan@usm.my](mailto:cygan@usm.my) (C.-Y. Gan).

have an efficient and high interaction effect on both the polar and non-polar ends of protein and starch constituents. The ability of solvents to interact with microwave energy can, therefore, be further improved by the use of mixtures of solvents. The dipole moment of the binary mixture influences the affinity and ability of the solvents to absorb the energy generated from the microwave electric and magnetic field rotation (Surat et al., 2012). Take, for instance, the mixture of ethanol and water has been reported to significantly absorb a sufficient amount of energy from the microwave electric field due to their high dielectric constant (63.18). Therefore, the binary mixture of ethanol and water was used in order to extract the polar and non-polar ends of the starch and protein in the seed powder.

The high nutritional properties of *Artocarpus heterophyllus* seed wastes can be adequately harnessed through the use of suitable processing condition medium and bio-product characterization (Jiang et al., 2019). Although previous studies had investigated the biological functions and the optimization of the extraction process (Begum et al., 2014). However, the mechanistic and synergistic effects of the extraction process on the plant structure were rarely discussed, and this could be best explained through concise physicochemical characterization.

The microwave extraction process is such an efficient and effective method which works on the principle of interaction between extracting solvents and the electromagnetic dipole field rotation (Silva et al., 2016). One of the merits of microwave techniques is the even and volumetric distribution of heat and mass transfer within the heating medium (Yuan and Macquarrie, 2015). This is an important advantage over the conventional methods of extraction such as maceration, Soxhlet extractions, sonication, in which the transfer of heat and mass is not uniform mostly from the region of higher temperature to a region of lower temperature (Veggi et al., 2013). The microwave extraction method is, therefore, a better approach combining the multi-directional electromagnetic radiation and conventional heating with shorter irradiation time, lower degradation, low solvent consumption, and high-quality extract (Paunović et al., 2014). Addressing the principle of microwave extraction is indeed not sufficient without some kind of full idea of the structural and textural modifications that have occurred in the process of removing bioactive compounds from plant-based nutraceuticals products (Olalere et al., 2018a, b). The estimation of the surface area and pore volume of medicinal plants pre and post extraction is important to assess the structural deformation of the sample under examination. The data gathered will then be used as a foundation for the assessment of the efficiency of various extraction techniques in the processing of quality bioproducts. The physicochemical characterization methods are usually needed for standardizing, determining and maintaining the quality characteristics of herbal bio-products (Olalere et al., 2018a, b). Therefore the use of suitable extraction medium to a larger extent determine the stability, quality and shelf-life of herbal products (Kumar, 2016). To, therefore, assess the extent of damage or release of medicinal constituents of these herbal products, an appropriate use of physicochemical analytical techniques is succinctly of necessity (Brandão et al., 2016). This is of paramount important for herbal formulation and in ascertaining the quality and safety of any plant-based drugs candidates. Different analytical techniques can be deployed to characterize the bioactive constituents in plant-based medicine viz: thermo-gravimetric, calorimeter, scanning electron microscopy, x-ray diffraction, mass spectrometry, and Fourier transform infrared techniques etc. The main objective of this study is to obtain information obtained to establish useful parameters required for maintaining the quality and safety of jackfruit (*A. heterophyllus*) bio-products. This study carefully elucidated the morphological configuration, functional characteristics, thermal stability and microchemical profile of raw and vegetative extracts from *A. heterophyllus* seed wastes using sets of physicochemical techniques. The output results obtained via Fourier transform infrared spectroscopy (FTIR), scanning electron microscopy (SEM), thermogravimetry (TGA) and liquid chromatographic mass spectrometry (LCMS QToF) obtained provided

information on the stability, standardization, morphology and chemical composition of the raw and vegetative bioactive extracts.

## 2. Materials and methods

### 2.1. Microwave extraction and extract preparation

The jackfruit (*A. heterophyllus*) fruits were procured from the local market in Gelugor, Penang Malaysia. The fresh seed was open air-dried to constant weight for one week and then crushed into finely divided powder using a commercial blender. The powder sample was clarified into a constant 0.105 mm particle size at an estimated moisture content of 8% before the extraction process was initiated. The microwave extraction of the powder sample was conducted using 1.0 g of the sample immersed in 100 mL of ethanol using an ETHOS-Milestone extractor (ATC-FO-300, North America). The output mixtures was filtered using vacuum pump and thereafter evaporated at under vacuum to obtain a semi-solid oleoresin extract, which was later spray-dried (B-290-model, Switzerland) under the feed flow rate of 12 mL/min, the inlet temperature of 150 °C, the outlet temperature of 80 °C, airflow rate of 600 L/h and pressure of 20 psi. The bio-product was refrigerated at 4 °C for further phytochemical characterization and micro-surface elucidation.

### 2.2. Taguchi optimization design

In this study, three extraction factors were considered and these include the extraction time ( $x_1$ ), microwave power ( $x_2$ ), extraction temperature ( $x_3$ ) and sample-to-solvent ratio ( $x_4$ ). The orthogonal Taguchi design was used for the determination of the significant relationship between the extraction variables and the response function which is the extraction percentage yield (Y). The corresponding lower (-1), middle (+0) and upper (+1) coded level were selected around the power setting of 450 W, extraction time of 10 min, and extraction temperature of 60 °C (Koh et al., 2014). The three selected coded levels (-1, 0, +1) for each factor include  $x_1$  (5, 8, 10) min,  $x_2$  (400, 450, 500) W, and  $x_3$  (40, 50, 60) °C. A binary mixture of ethanol and water (60%) was used as an extracting solvent. The response function (extraction percentage yield (Y)) is expressed using the larger-is-better signal to noise ratio model with the four independent variables as presented in Eq. (1).

$$SNR_{(Large-the-better)} = -10 \cdot \log 10 \left\{ \left( \frac{1}{y} \right)^2 / n \right\} \quad (1)$$

where n is the number of observation and y is the observed data. A higher value of larger-is-better and lower smaller-is-better SN-ratio respectively indicate that the response set is a good predictor of the extraction process. On the overall, the Taguchi design involves minimal experimental runs, thereby reducing the time and cost of the sample been investigated (Abdurahman and Olalere, 2016).

### 2.3. Characterization

#### 2.3.1. FTIR analysis

The surface chemistry and functional characteristics of the microwave *A. heterophyllus* extracts were characterized using an iS5 iD7-ATR-model spectrometer by the method used by Olalere et al. (2017). Briefly, the infrared spectra were obtained within the scanning range of 500–4000  $\text{cm}^{-1}$ . The output spectra of the sample were relayed and displayed with the aid of OMNIC software attached to the spectrometer.

#### 2.3.2. TGA and SEM analysis

The *A. heterophyllus* raw samples and the vegetative extracts were subjected to morphological analysis using a Fei Quanta 450 scanning electron microscope. The monograph of the raw sample and the extracts were captured at magnifications of 300 and 200

$\mu\text{m}$ , respectively. Moreover, the thermal stability of the extracts (8.2230 mg) was tested using a TG-DTA (Model Q500-V6.4, Germany) in an alumina pan between 30 to 500 °C temperature. The system was set under atmospheric nitrogen ( $\text{N}_2$ ) at a heating rate of  $10\text{ }^\circ\text{C min}^{-1}$  and gas flow rate of  $20\text{ mL min}^{-1}$ . Other parameters values used in the TGA protocol include an  $\text{N}_2$  balance purge of 60 ml/min,  $\text{N}_2$  sample purge of 40 ml/min.

### 2.3.3. Tentative chemical profiling

The tentative identification of phenolic compounds in the *A. heterophyllum* extracts was conducted using a Vion Ion Mobility LC-Q-TOF-MS (Waters, USA) as described by Olalere et al. (2018a), b. Briefly, the chromatographic ACQUITY UPLC HSS T3-column was used for separation with the dimension 2.1 by 100 mm and a particle size of 1.8  $\mu\text{m}$ . The mobile phase was made up of 0.1 % formic acid and 0.1 % of formic acid in acetonitrile. The detail of the LC-Q-TOF-MS protocol has been elaborated by Olalere et al. (2018a), b.

## 3. Results and discussion

### 3.1. Determination of optimum condition

The orthogonal optimization design (Table 1) was employed to determine the combined effects of three parameters on the extraction yield. The optimal extraction condition was selected based on the largest-donating-rule which states that for each extraction variables under consideration, the parameter with the largest response (maximal) and highest SNR should be selected as the optimal response settings (Olalere et al., 2019). Therefore, the optimal condition of extraction was achieved at 5 min extraction time, 450W microwave power and 50 °C of extraction temperature. Under this condition, the optimal extraction yield of the microwave extraction was 17.34 (mg/g) % at the signal-to-noise (SNR)

ratio of 24.78. This condition provided a combination of parameters that jointly achieved a higher extraction yield.

### 3.2. Statistical analysis of mean and variance

The significant contribution of each extraction parameters on the extraction yield was determined and quantified from extremum difference computation. The value generated from the extremum difference ( $\beta_{\text{max}} - \beta_{\text{min}}$ ) was used for the determination of mean effects or the significant contribution of the three microwave extraction parameters. From Table 2, the ranking of each extraction factor was determined from the computed  $\beta_{\text{max}} - \beta_{\text{min}}$  obtained from the average SNR.

Meanwhile, Figure 1 shows optimal SNR of 22.63 at level-1 of the extraction time (5min), 23.40 at level-2 of the microwave power (450 W), and 22.32 at level-2 of the extraction temperature (50 °C). The decreasing order of significance of the three extraction variables to the percentage yield is  $x_2 > x_1 > x_3$ . The decreasing order of contribution of the variables shows microwave power as the largest contributor for optimum extraction, while the extraction time has the least contribution to the process. Therefore good quality characteristics, a higher microwave power, lower extraction time and moderate heat are required for optimal extraction yield (Alara et al., 2017).

### 3.3. Physicochemical characterization of the raw and crude extracts

#### 3.3.1. Functional group fingerprint

The emission spectrum and the corresponding assigned frequency of vibration for the *A. heterophyllum* seeds extracts are presented in Figure 2 and Table 3. The appearance of the O–H group ( $3246\text{ cm}^{-1}$ ) is due to the stretching of the phenolic components of the microwaved extract. According to Barua and Boruah (2009), the region around the wavenumber  $3246\text{ cm}^{-1}$  region indicated the carbohydrate component in the jackfruit seed extracts. This confirmed the assertion of Koh et al. (2014) who

**Table 1.** Taguchi experimental design ( $L_9$ ) for the determination of optimal extraction conditions.

$x_1$ (min)	$x_2$ (W)	$x_3$ (°C)	Y (mg/g %)	Signal-to-noise ratio (SNRA1)
1	1	1	11.42	21.1533
1	2	2	17.34	24.7810
1	3	3	12.54	21.9660
2	1	2	10.93	20.7724
2	2	3	14.87	23.4462
2	3	1	11.03	20.8515
3	1	3	10.74	20.6201
3	2	1	12.53	21.9590
3	3	2	11.07	20.8830

**Table 2.** Analysis of variance and means for SN ratios (Larger is better).

Level	$x_1$ (min)	$x_2$ (W)	$x_3$ (°C)
$\beta_1$	22.63	20.85	21.32
$\beta_2$	21.69	23.40	22.15
$\beta_3$	21.15	21.23	22.01
Delta	1.48	2.55	0.82
Rank	2	1	3
Seq SS	3.37	11.31	1.17
Adj SS	3.37	11.31	1.17
Adj MS	1.68	5.65	0.59
F	8.35	28.05	2.91
p-value	0.007 <sup>s</sup>	0.034 <sup>s</sup>	0.256

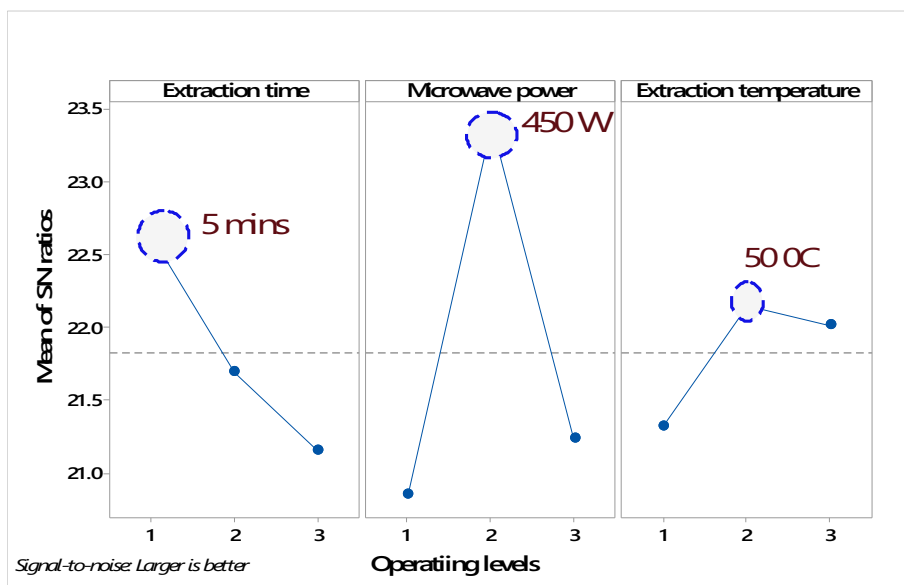


Figure 1. Mean effect analysis of SNR showing the factors' significant contribution.

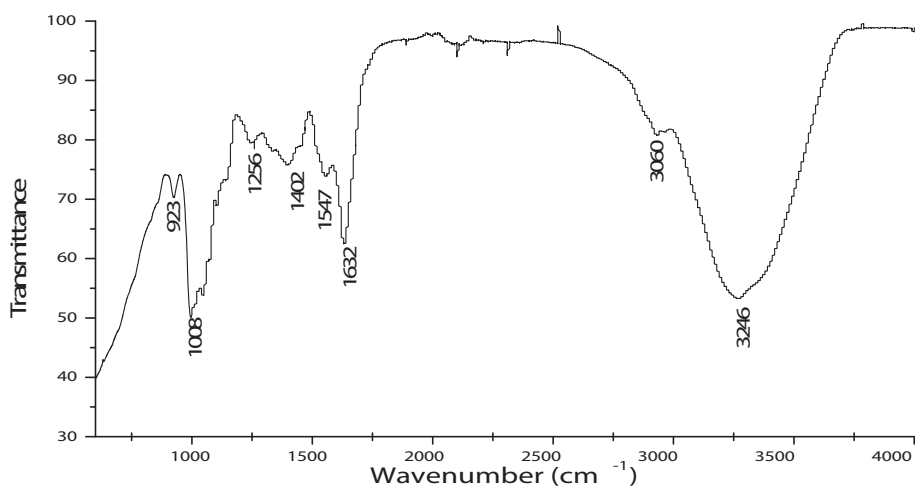


Figure 2. FTIR analysis of jackfruit seed (*A. heterophyllum*) seeds wastes.

reported the major components of jackfruit seeds waste as carbohydrate and protein. The region within the  $3060\text{ cm}^{-1}$  represented the stretching vibration of the amide group N–H group, while the wavelength at  $1638\text{ cm}^{-1}$  is the C=O stretching vibration of dis-substituted amide. The amide

group indicated the protein content which is directly linked with the carbonyl group (C=O) as supported by Theophanides (2012).  $1547$ , and  $1402\text{ cm}^{-1}$  represent the asymmetric deformation of the  $\text{CH}_2\text{--CH}_2$  bonds. The band at  $1256\text{ cm}^{-1}$  corresponds to the aliphatic oxide of phosphorus

Table 3. Vibrational frequencies of microwaved jackfruit seed extracts.

Frequency ( $\text{cm}^{-1}$ )	Bond identified	Peak attribute
$3246^c$	O–H	Phenolic stretching of O–H bond
$3060^b$	C–H	Amide group: Stretching of N–H bond
$1638^a$	C=O	Stretching of C=O bond
$1547^b$	$\text{CH}_2 = \text{CH}_2$	Stretching of $\text{CH}_2 = \text{CH}_2$ bond
$1402^b$	$\text{CH}_2 = \text{CH}_2$	Asymmetric deformation of $\text{CH}_2 = \text{CH}_2$
$1256^b$	P=O	Stretching of P=O bond
$1008^a$	C–O	Stretching of C–O bond
$923^b$	C–H	In-plane bending of C–H bond

<sup>a</sup> Sharp peak strength.

<sup>b</sup> Weak peak strength.

<sup>c</sup> Broad peak.

(P=O) stretching (Barua and Boruah, 2009). Moreover, the wavelength at  $1008\text{ cm}^{-1}$  represents the carbohydrates functionality of the C–O bond, whereas the  $923\text{ cm}^{-1}$  is attributed to the in-plane bending of the C–H group.

### 3.4. Textural characteristics and thermal stability of the *A. heterophyllum* matrix

Figure 3 (a) and (b) showed the morphological transformation in the microstructure of *A. heterophyllum* seeds before and after the microwave treatment. The raw *A. heterophyllum* seeds (Figure 3a) exhibited an elongated smooth surface which suggests an intact microstructural area with tiny granules. The application of a multi-directional microwave heat resulted in the disorientation of the structure which led to the formation of starch globules with a characteristics circular and overlapping structure (Figure 3b). This is consistent with the monographs obtained by Madruga et al. (2014) for crude extracts obtained from the Brazilian jackfruit seeds. The result obtained shows that irrespective of the geographical location where the jackfruit is grown, the shapes of the starch granules are the same. The remarkable difference in the sizes and conspicuousness of the circular starch granules grown in different parts of the world is largely dependent on the method of processing and the parameter settings during the process of extraction. This is evident in the monograph obtained by Madruga et al. (2014) and the results of this investigation which shows bigger granular sizes as compared to previous studies. The result of this study indicates that the use of microwave extraction technology produced increased the efficiency of extraction with lower degradation of the thermal labile constituents. Therefore the extraction of jackfruits using the microwave technique reduces the extraction time, higher yield, improved selectivity, and produced good quality extracts as buttressed by Koh et al.,(2014).

The thermal degradation of the *A. heterophyllum* samples undergoes three important degradation stages. The first thermal decomposition occurred within the temperature difference of  $68.43\text{ }^{\circ}\text{C}$ . At this stage, an estimated mass loss of  $2.023\text{ mg}$  was recorded which accounted for  $24.60\text{ per cent}$ . Also, the second stage exhibited an averagely high-temperature difference of  $180.57$  and a mass loss of  $0.6658\text{ mg}$  accounting for just  $8.097\text{ percentage loss}$ . This stage has been predicted to release the thermo-sensitive constituents in the *A. heterophyllum* sample (Brandão et al., 2016). The third stage has the largest degradation temperature

difference of  $258.03\text{ }^{\circ}\text{C}$  with  $46.60\text{ %}$  decomposition. The wide temperature difference could be attributed to the release of higher molecular constituents. According to Brandão et al. (2016) this third stage is regarded as the terminal of thermal degradation of any medicinal plant which is largely associated with the thermal degradation of carbohydrates and other organic compounds present in the plant matrix. Beyond this stage, the sample was completely lost to pyrolysis and degraded into a completely denatured hydro char and oxides (Brandão et al., 2016). The summary of the degradation profile is illustrated in Table 4.

### 3.5. Identification of bioactive constituents

The LCMS analysis was employed for the identification of bioactive constituents in the oleoresin extracts of *A. heterophyllum* seeds wastes. The results obtained identified a total of 90 and 148 bioactive constituents at positive and negative ESI- modes as presented in Tables 5 and 6, respectively. The identified bioactive constituents are largely responsible for the nutritional and medicinal potential of the valorised *A. heterophyllum* wastes. Figure 4 (a) and (b) contained the summary of the identified representative food and medicinal bioactive compounds with their mass-to-charge ratio (m/z), retention time and adducts. An important alkaloid identified from the positive ionization mode is the pungent shogaols (m/z =  $543.20$ , RT =  $5.93\text{ min}$ ) which is similar to the established piperine and capsaicin from chilli and black pepper (Semwal et al., 2015). This is an important spicy compound with flavouring attribute which could be a potential alternative for food preservations and as an anti-inflammatory agent when isolated as a single pure compound (Li et al., 2019). Moreover, the presence of other secondary alkaloids such as Dendrocandine F (m/z =  $315.13$ , RT =  $6.72\text{ min}$ ) (Yang et al., 2018), Yakuchinone A (m/z =  $357.17$ , RT =  $12.38\text{ min}$ ) (Sur et al., 2019), Aspidinol (m/z =  $269.10$ , RT =  $6.45\text{ min}$ ) (Wang et al., 2016), Saponin PA (m/z =  $853.46$ , RT =  $10.89\text{ min}$ ) (Xu et al., 2013) confirmed the activities of *A. heterophyllum* as anti-tumour agents which makes them potential drug candidates against cancerous cells.

Moreover, the slightly bitter taste of the seed could be attributed to the presence of phenolic constituents known as isomangiferin (m/z =  $421.0754$ , RT =  $0.57\text{ min}$ ) which is largely present in coffee leaves in most herbal tea as reported by Alexander et al. (2019) and Chen et al. (2019). Also, the presence of bioactive constituents such as Euparin (m/z =  $261.0744$ , RT =  $4.23\text{ min}$ ) (Frišćić et al., 2019), Gingerone (m/z =

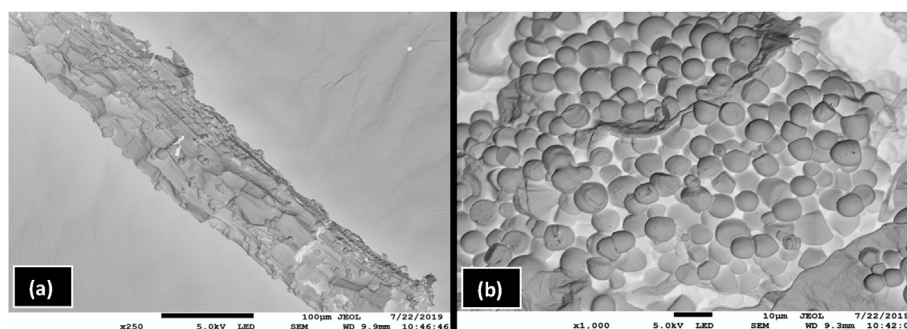


Figure 3. SEM monograph of *A. heterophyllum* seeds (a) raw sample (b) spray-dried extract.

Table 4. TGA/DTA analysis of the *A. heterophyllum* extracts at different degradation region.

Degradation stages	$\Delta T\text{ (}^{\circ}\text{C)}$	$\Delta m\text{ (mg)}$	Percentage mass loss %	Regional attributes
Stage 1	68.43	2.0230	24.60	Moisture removal
Stage 2	180.57	0.6658	8.097	Released of thermo labile content
Stage 3	258.03	0.078	46.60	Higher molecular content

**Table 5.** Tentative identification of food bioactive from *A. heterophyllum* seeds extracts in negative (-ve) ESI-mode.

Compound	Observed m/z	Observed RT (min)	Adducts
Dendrocandian F	543.2064	6.72	-H, +HCOO
Yakuchinone A	357.1732	12.38	+HCOO
1,5-Dihydroxy-2,3,4,7-tetramethoxyxanthone	393.08	4.45	+HCOO
Isosakuranetin-7-rutinoside	639.1923	4.95	+HCOO
Gingerone	239.0927	6.25	+HCOO
Yakuchinone A	357.1739	18.54	+HCOO
Isomangiferin	421.0754	0.57	-H
Genistein_1	269.0462	14.25	-H
Kaempferol 3-O- $\beta$ -D-glucuronopyranosyl methyl ester	521.0963	4.24	+HCOO
Euparin	261.0744	4.23	+HCOO
Patuletin-7-O-[6''-(2-methylbutyryl)]-glucoside	563.1409	10.16	-H
Aspidinol	269.1031	6.45	+HCOO
Osmanthuside H	477.1607	6.2	+HCOO
Yakuchinone B	355.1584	12.53	+HCOO
(2R,3R)-Taxifolin-7-O- $\alpha$ -L-rhamnopyranosyl-(1 $\rightarrow$ 6)- $\beta$ -D-glucopyranoside	611.1617	8.88	-H
Silydianin	481.1171	1.28	-H
Dendrocandian B	527.1965	16.41	+HCOO
Pelargonidin 3,5-diglucoside	675.1337	0.82	+HCOO
Moracin C	309.1132	16.6	-H
3-(4-Hydroxyphenyl)-4-methoxy-2,7-dihydroxy-9,10-dihydrophenanthrene	347.1319	16.69	-H, +HCOO
Cyclopseudohypericin	547.0643	10.31	+HCOO, -H
Limocitrin-3,7-O- $\beta$ -D-glucopyranoside	715.1775	4.94	+HCOO
Cyclopseudohypericin	547.0643	11.93	+HCOO, -H
Kaempferol 3- $\alpha$ -L-dirhamnosyl-(1 $\rightarrow$ 4)- $\beta$ -D-glucopyranoside	593.1515	10.53	-H
Kushenol G	501.173	7.07	+HCOO
Saponin PA	853.461	10.89	-H
Malvidin-3-O-(6-O-acetyl- $\beta$ -D-glucopyranoside)-5-O- $\beta$ -D-glucopyranoside	695.1875	0.84	-H
Euparin	261.0746	7.07	+HCOO
Kaempferol 3- $\alpha$ -L-dirhamnosyl-(1 $\rightarrow$ 4)- $\beta$ -D-glucopyranoside	639.1567	8.58	+HCOO
Gingerone	239.0924	5.92	+HCOO
Euparin	261.0746	7.07	+HCOO
Yakuchinone B	355.1582	12.65	+HCOO
6''-O-p-Hydroxybenzoyliridin	641.1542	1.15	-H
Aloeresin	439.1221	18.58	+HCOO
Isomangiferin	421.0754	0.57	-H
Blestrin B	527.1672	7.66	+HCOO
Khellol- $\beta$ -D-glucoside	453.1039	18.58	+HCOO
Obovatol	327.1269	15.95	+HCOO
Kukoamine A	575.307	15.88	+HCOO
Gingerone	239.0922	4.56	+HCOO
Cistanoside B	813.2828	7.66	-H
Isoanhydrocaritin	429.1542	3.91	+HCOO
Sophoflavescenol	429.1542	3.91	+HCOO
Osmanthuside H	431.1559	5.76	-H
3,4,2'-Trihydroxychal-cone-4'-O- $\beta$ -D-glucopyranoside	479.1177	18.65	+HCOO
5,7,2'-Trihydroxy-flavanone-4'-O- $\beta$ -D-glucoside	449.1091	6.6	-H
Sagittatoside B	645.216	10.79	-H
Licurazide	549.1596	4.96	-H
Gingerone	193.0877	16.54	-H
Norkurainol	485.1773	6.45	+HCOO
$\beta$ -Hydroxyacteoside	685.1988	4.95	+HCOO, -H
(+)-Catechin-pentaacetate	545.1258	4.85	+HCOO
Osmanthuside H	431.1556	5.14	-H
Gingerone	239.0922	4.23	+HCOO
Sagittatoside B	645.2166	10.43	-H
(3R,4R)-3,4-trans-7,2',3'-Trihydroxy-4'-methoxy-4-[(3R)-2',7-dihydroxy-4'-methoxy-isoflavan-5'-yl]-isoflavan	557.1778	8.1	-H
Aloeresin C	701.2117	16.63	-H
Magnolol	311.1314	16.19	+HCOO

(continued on next page)

Table 5 (continued)

Compound	Observed m/z	Observed RT (min)	Adducts
Osmanthuside H	431.1558	4.4	-H
3-Hydroxy baicalein	285.0405	12.77	-H
7-Hydroxy-1-methoxy-2-methoxyxanthone	285.0405	12.77	-H
(3R,4R)-3,4-trans-7,2',3'-Trihydroxy-4'-methoxy-4-[(3R)-2',7-dihydroxy-4'-methoxy-isoflavan-5'-yl]-isoflavan	557.1773	8.3	-H
Tubuloside E	695.2187	12.04	+HCOO
Odoratin-7-O-β-D-glucoside	477.139	4.85	+HCOO
Sagittatoside B	645.2165	10.64	-H
Tiliroside	593.1303	16.64	-H
(3R,4R)-3,4-trans-7,2',3'-Trihydroxy-4'-methoxy-4-[(3R)-2',7-dihydroxy-4'-methoxy-isoflavan-5'-yl]-isoflavan	557.178	7.26	-H
6-Methoxy-2-[2-(4'-methoxyphenyl) ethyl] chromone	325.1472	17.24	-H
(-)-Epiafzelechin-3-O-(6''-O-acetyl)-β-D-allosepyranoside	523.144	4.85	+HCOO, -H
6-Aldehyde-7-methoxy-isoochloretin B	353.1031	16.65	-H
Blestrin B	527.1669	8.65	+HCOO
Sanggenon J	487.2079	16.46	-H
Feroxin A	401.1448	4.23	+HCOO
Gingerone	239.0921	4.9	+HCOO
Darendoside A	431.1558	5.33	-H
Osmanthuside H	431.1558	5.33	-H
Sagittatoside B	645.2163	10.25	-H
(3R,4R)-3,4-trans-7,2',3'-Trihydroxy-4'-methoxy-4-[(3R)-2',7-dihydroxy-4'-methoxy-isoflavan-5'-yl]-isoflavan	557.1772	9.15	-H
Honokiol	311.1295	16.55	+HCOO
Magnolol	311.1295	16.55	+HCOO
Yakuchinone B	355.1586	17.44	+HCOO
Sagittatoside B	645.2164	9.68	-H
Sagittatoside B	645.2161	10.15	-H
Sagittatoside B	645.2163	9.95	-H
Feroxin A	401.1447	4.89	+HCOO
6-Methoxy-2-[2-(4'-methoxyphenyl) ethyl] chromone	325.1464	18.58	-H
Sagittatoside B	645.2162	9.53	-H
Feroxin A	401.1452	6.45	+HCOO
Feroxin A	401.1448	4.23	+HCOO

Table 6. Tentative identification of food bioactive from *A. heterophyllum* seeds extracts in positive ESI-mode.

Component name	Observed m/z	Observed RT (min)	Adducts
Meliadoside B	351.1053	4.9	+Na
Homoarbutin	287.1098	3.4	+H
Osmanthuside H	455.1526	6.29	+Na
Octahydrocurcumin	399.1775	14.15	+Na
Khellol-β-D-glucoside	409.1105	6.45	+H
Pseudoaspidin	499.1779	8.09	+K
Irisolidone	353.0393	0.76	+K
5,3',5'-Trihydroxy-6,7,4'-trimethoxy flavone	361.0893	6.58	+H
Bavachinin	377.1133	4.83	+K
Aloeresin G	539.1888	7.51	+H
Cimidahurine	317.1204	5.24	+H
Albaspidin AA	405.1523	14.55	+H
Digupigan A	473.106	6.6	+K
Aloeresin G	539.1907	7.8	+H
Tribulusamide A	625.2496	10.5	+H
Cyclomorusin	419.1523	3.83	+H
Isoaloesin D	557.1979	9.55	+H
Phellochinin A	519.1851	6.03	+H
Shogaol	315.1334	4.83	+K
7-Hydroxy-3-(4'-hydroxybenzylidene)-chroman-4-one	269.081	16.58	+H
Arbutin	273.0943	1.93	+H
Kushenol E	463.1534	5.57	+K
Kushenol M	509.2565	9.81	+H

(continued on next page)

Table 6 (continued)

Component name	Observed m/z	Observed RT (min)	Adducts
Isomangiferin	423.0895	7.24	+H
Noranhycaritin	371.1457	8.94	+H
Salidroside	323.1099	4.53	+Na
Meliadanoside B	351.1057	5.98	+Na
Licoricone	405.128	2.33	+Na
Compound	Observed m/z	Observed RT (min)	Adducts
Cyclomorusin	419.1521	4.3	+H
Kuwanon P	605.1768	0.97	+Na
Gigantol	261.1098	15.16	+H
Sanggenon J	511.2137	8.31	+Na
Isomangiferin	423.0903	6.24	+H
(1R,2S,3R,6'R,7'R)-3, 7'-Bis(3,4-dihydroxy-phenyl)-1,1',2,2',3,3', 4,4'-octahydro-1, 1'-binaphthyl-2,2',4',6,6',8-hexaol	575.1889	14.7	+H
1-(4-Hydroxybenzyl)-4-methoxy-2,7-dihydroxyphenanthrene	347.1311	4.98	+H
(3R,4R)-3,4-trans-7,2',3'-Trihydroxy-4'-methoxy-4-[(3R)-2',7-dihydroxy-4'-methoxy-isoflavan-5'-yl]-isoflavan	559.1918	7.26	+H, +Na
Apigenin-6-C-glucosylglucoside	595.1667	10.52	+H, +Na
Undulatoside A	377.085	6.33	+Na
Cistanoside H	505.1867	18.62	+H
Tubuloside B	689.2061	9.35	+Na, +K
Khellol-β-D-glucoside	409.1103	5.78	+H
Sec-O-glucosylhamaudol	439.1578	7.78	+H
Mulberrofuran C	603.1607	6.18	+Na
Sophoflavescenol	423.1176	4.9	+K
Kushenol H	511.1713	8.65	+K
Salidroside	323.1094	3.58	+Na
Isomangiferin	423.0896	6.57	+H
Mulberrofuran D	447.2567	16.34	+H
Sophoflavescenol	385.1622	16.38	+H
Phlorofucofuroeckol A	603.0722	0.97	+H
Albaspidin AA	405.1518	14.83	+H
Dendrocandin F	545.2183	8.53	+H
Digupigan A	457.1318	10.49	+Na
Yakuchinone B	349.1182	11.37	+K
Cistanoside A	801.2823	3.73	+H
Cistanoside B	837.2803	7.66	+Na, +K
Sophoraisoflavone A	353.1011	16.74	+H
Cimidahurine	317.1204	4.54	+H
Forsythoside D	501.1576	4.27	+Na, +K
Cimidahurine	317.1202	3.92	+H
Daidzein	255.0657	16.62	+H
Kuwanon K	693.2292	2.12	+H
1-(4-Hydroxybenzyl)-4-methoxy-2,7-dihydroxyphenanthrene	347.1305	5.62	+H
Dendrocandin F	545.2183	7.48	+H
(-)-Epiatzelechin-3-O-(6''-O-acetyl)-β-D-allosepyranoside	479.1547	4.84	+H
Shogaol	315.1339	4.72	+K
Bavachalcone	363.0964	5.39	+K, +Na
4-(4'-Hydroxy-3',5'-dimethoxyphenyl)-3-buten-2-one	223.0965	4.9	+H
Castalagin	935.0801	18.61	+H
Undulatoside A	377.0842	5.4	+Na
Isomangiferin	423.0896	6.57	+H
N-Dihydro-caffeoyltyramine	302.1388	11.23	+H
Kuwanon P	583.2007	7.57	+H
Shogaol	277.1772	15.27	+H
Kushenol H	473.2157	15.01	+H
Meliadanoside A	377.1413	3.82	+H
1,5-Dihydroxy-2,3,4,7-tetramethoxyxanthone	349.0891	4.45	+H, +Na
Sec-O-glucosylhamaudol	439.1575	6.94	+H
3',4'-Dimethoxy-isoflavan-7,2'-di-O-β-D-glucoside	627.2278	8.13	+H
Koburaside	333.1156	3.81	+H, +Na

(continued on next page)

Table 6 (continued)

Component name	Observed m/z	Observed RT (min)	Adducts
Sanggenon G	695.2511	7.06	+H
2,6-Bis(4-hydroxyphenyl)-3',5-dimethoxy-3-hydroxybibenzyl	471.22	14.22	+H
2',6'-Dihydroxy-4,4'-dimethoxydihydrochalcone	303.1203	13.21	+H
Homoarbutin	287.1099	3.76	+H
Cimidahurine	317.1201	5.06	+H, +Na
Kushenol H	495.2004	15.52	+Na
2,7-Dihydroxy-1-(p-hydroxybenzoyl)-4-methoxy-9,10-dihydrophenanthrene	363.1256	2.68	+H
Salidroside	301.1256	5.39	+H
Blestrin B	483.1843	4.98	+H
Osmanthuside H	433.1674	4.34	+H
Osmanthuside H	455.1523	4.13	+Na
Sanggenon G	695.2529	8.12	+H
(1R,2S,3R,6'R,7'R)-3,7'-Bis(3,4-dihydroxy-phenyl)-1,1',2,2',3,3',4,4'-octahydro-1,1'-binaphthyl-2,2',4',6,6',8-hexaol	575.1886	14.19	+H
Isoaloeresin D	557.1977	6.76	+H
Osmanthuside H	455.1521	4.41	+Na, +K
2-Octylphenol	229.1545	0.54	+Na
Neoisostilbin	451.122	5.52	+H
Osmanthuside H	455.1521	5.15	+Na
Cimidahurine	317.1208	7.75	+H
Blestrin B	483.1838	12.24	+H
Shogaol	315.1339	5.93	+K
Furoaloesone	257.0807	16.56	+H
Blestriarene B	481.1679	5.21	+H
Obtustylene	263.1023	2.33	+Na
(3R,4R)-3,4-trans-7,2'-Dihydroxy-4'-methoxy-4-[(3R)-2',7-dihydroxy-4'-methoxy-isoflavan-5'-yl]-isoflavan	543.2052	6.09	+H
Dendrocandin B	483.2058	16.41	+H, +Na
Sanggenon J	489.23	12.1	+H
5,7,4'-Trihydroxy-8,3'-diprenylflavone	429.1715	5.92	+Na, +K
Icariin	677.2415	8.78	+H
3-Hydroxy baicalin	287.055	12.76	+H
Fisetin	287.055	12.76	+H
Cimidahurine	355.0798	13.52	+K
Forsythoside D	501.1582	5.95	+Na, +K
Furoaloesone	257.0807	16.55	+H
Liquiritigenin	257.0807	16.55	+H
(3R,4R)-3,4-trans-7,2',3'-Trihydroxy-4'-methoxy-4-[(3R)-2',7-dihydroxy-4'-methoxy-isoflavan-5'-yl]-isoflavan	559.1919	9.15	+H, +Na
Sanggenon J	489.231	11.67	+H
Dendrocandin F	545.2197	6.72	+H
Blestrin B	487.2152	8.38	+H
$\beta$ -Hydroxyacteoside	641.2071	4.93	+H
Mulberrofuran C	603.1608	6.18	+Na, +K
5,7,4'-Trihydroxy-8,3'-diprenylflavone	407.1882	6.61	+H
Osmanthuside H	455.1521	5.33	+Na, +H
2-Octylphenol	229.1548	1.54	+Na
Sanggenon J	489.2302	11.8	+H
(-)-Epiafzelechin-3-O-(6''-O-acetyl)- $\beta$ -D-allosepyranoside	479.1548	4.83	+H
Sanggenon A	437.1629	2.66	+H
Tellimagrandin II	961.0952	18.61	+Na
Sagittatoside B	647.2313	10.63	+H, +Na
Irilone	299.0548	16.65	+H
Kushenol U	461.171	5.93	+K
6-Methoxy-2-[2-(4'-methoxyphenyl) ethyl] chromone	349.139	3.87	+Na
Irilone	299.0548	16.65	+H
1-(4-Hydroxybenzyl)-4-methoxy-2,7-dihydroxyphenanthrene	347.131	5.39	+H
(3R,4S)-3,4-Dihydroxy-3-(3',4'-dimethoxybenzyl)-7-methoxy-chroman	347.1464	13.92	+H
Mulberrofuran O	647.2314	10.25	+H, +K, +Na
Sec-O-glucosylhamaudol	439.1578	7.78	+H
Sagittatoside B	647.2316	10.15	+H, +Na

(continued on next page)

Table 6 (continued)

Component name	Observed m/z	Observed RT (min)	Adducts
Sagittatoside B	647.2313	9.67	+H, +Na
Mulberrofuran O	647.2314	9.94	+H, +K, +Na
Sagittatoside B	647.2314	9.94	+H, +Na
(±)-Isoduartin	355.1174	16.64	+Na
Sanggenon H	355.1174	16.64	+H
5,7,4'-Trihydroxy-8,3'-diprenylflavone	407.1888	7.01	+H, +K, +Na
Sagittatoside B	647.2316	9.53	+H, +Na
Glabrol	393.2094	6.09	+H
Glabrol	393.2096	6.89	+H

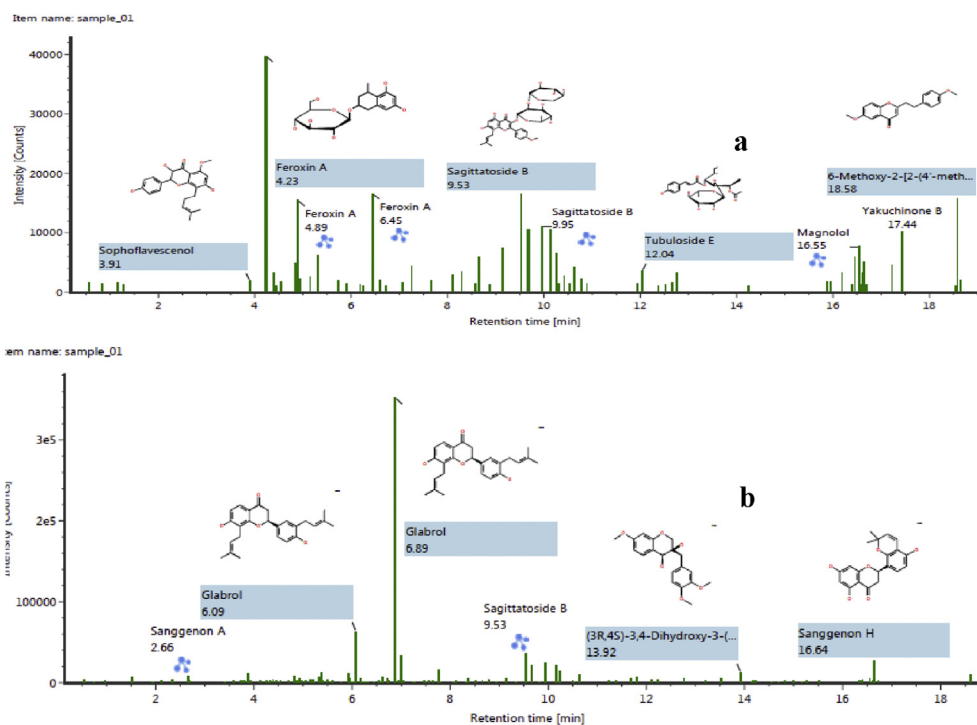


Figure 4. Tentatively identified representative compounds from LCMS-QToF (a) Negative (-ve) ESI mode (b) Positive (+ve) ESI mode.

261.07, RT = 5.92min), Kukoamine A ( $m/z = 575.30$ , RT = 15.88 min), Aloeresin ( $m/z = 439.12$ , RT = 18.58 min), Sophoflavescenol ( $m/z = 429.15$ , RT = 3.91 min), are largely responsible for the antioxidant potential of *A. heterophyllum* seeds extracts. Specifically, Jung et al. (2011) reported the antidiabetes activities of the flavonols Sophoflavescenol from *Sophora flavescens* and their structure relationship activity. Dalko et al. (2014) investigated the anti-inflammatory properties of Gingerone and their inherent cosmetic use as an anti-ageing agent. Kukoamine A, Euparin and Aloeresin are other components with anti-inflammatory properties as reported by Wang et al. (2020), Xiao et al. (2020) and Adom et al. (2020).

#### 4. Conclusion

The physical and chemical characteristics of *A. heterophyllum* seeds were elucidated to determine the functional group, degradation profile, and textural characteristics of *A. heterophyllum* seeds from microwave heating effects. In this study, the microwaved *A. heterophyllum* seed wastes were characterized using a set of analytical protocols vis: FTIR, LC-MS/QToF, TGA and FESEM. The results obtained showed a remarkable irreversible impact of the electromagnetic microwave radiation on the texture, thermal stability and phenolic exudation of the sample. The combined effects of the extraction method determined to a larger extent

the medicinal and nutritional functionality of the *A. heterophyllum* seeds with potential application in the determination of quality characteristics of the extracts in food and drug applications.

#### Declarations

##### Author contribution statement

Olusegun A. Olalere: Conceived and designed the experiments; Performed the experiments; Wrote the paper.

Chee-Yuen Gan: Analyzed and interpreted the data; Wrote the paper. Hamid N. Abdurahman: Contributed reagents, materials, analysis tools or data.

Oladayo Adeyi, Mani M. Ahmad: Analyzed and interpreted the data.

##### Funding statement

This work was supported by Analytical Biochemistry Research Center (ABrC), Universiti Sains Malaysia (Postdoctoral Fellowship Scheme).

##### Competing interest statement

The authors declare no conflict of interest.

## Additional information

No additional information is available for this paper.

## References

- Abdurahman, N.H., Olalere, O.A., 2016. Taguchi-based optimization technique in reflux microwave extraction of piperine from black pepper. *Aust. J. Bas. Appl. Sci.* 10, 293–299.
- Adom, D., Sekyere, P.A., Krishnappa, M.K., 2020. The chemical constituents, anti-inflammatory, anti-oxidant, and ethnomedicinal properties of aloe barbadensis. In: *Ethnomedicinal Plant Use and Practice in Traditional Medicine*, pp. 181–198.
- Alara, O.R., Abdul Mudalip, S.K., Olalere, O.A., 2017. Optimization of mangiferin extracted from Phaleria macrocarpa fruits using response surface methodology. *J. Appl. Res. Med. Aromat. Plants* 5, 82–87.
- Alexander, L., de Beer, D., Muller, M., van der Rijst, M., Joubert, E., 2019. Bitter profiling of phenolic fractions of green Cyclopia genistoides herbal tea. *Food Chem.* 276, 626–635.
- Balamaze, J., Muyonga, J.H., Byaruhanga, Y.B., 2019. Physico-chemical characteristics of selected jackfruit (*Artocarpus heterophyllus* lam) varieties. *J. Food Res.* 8, 11.
- Barua, A.G., Boruah, B.R., 2009. Minerals and functional groups present in the jackfruit seed : a spectroscopic investigation. *Int. J. Food Sci. Nutr.* 55, 479–483.
- Begum, R., Aziz, M.G., Uddin, M.B., Yusuf, Y.A., 2014. Characterization of jackfruit (*Artocarpus heterophyllus*) waste pectin as influenced by various extraction conditions. *Agric. Agric. Sci. Procedia* 2, 244–251.
- Brandão, D.O., Guimarães, G.P., Santos, R.L., De Júnior, F.J.L.R., Da Silva, K.M.A., De Souza, F.S., Macêdo, R.O., 2016. Model analytical development for physical, chemical, and biological characterization of momordica charantia vegetable drug. *J. Anal. Methods Chem.* 1, 2016.
- Chen, X., Mu, K., Kitts, D.D., 2019. Characterization of phytochemical mixtures with inflammatory modulation potential from coffee leaves processed by green and black tea processing methods. *Food Chem.* 271, 248–258.
- Dalko, M., Saussay, S., Lo, S., 2014. Use of gingerone or derivatives thereof for reducing or delaying the signs of skin ageing. United States Patent Application 20140039064 218 (14/009).
- Fršićić, M., Jerković, I., Marijanović, Z., Dragović, S., Hazler Pilepić, K., Maleš, Ž., 2019. Essential oil composition of different plant parts from Croatian petasites albus (L.) gaertn. And petasites hybridus (L.) G.gaertn., B.mey. & scherb. (Asteraceae). *Chem. Biodivers.* 16.
- Jiang, Z., Shi, R., Chen, H., Wang, Y., 2019. Ultrasonic microwave-assisted extraction coupled with macroporous resin chromatography for the purification of antioxidant phenolics from waste jackfruit (*Artocarpus heterophyllus* Lam.) peels. *J. Food Sci. Technol.* 56, 3877–3886.
- Jung, H.A., Jin, S.E., Park, J.S., Choi, J.S., 2011. Antidiabetic complications and anti-alzheimer activities of sophoflavescenol, a prenylated flavonol from *Sophora flavescens*, and its structure–activity relationship. *Phyther. Res.* 25, 709–715.
- Koh, P.C., Leong, C.M., Noranizan, M.A., 2014. Microwave-assisted extraction of pectin from jackfruit rinds using different power levels. *Int. Food Res. J.* 21, 2091–2097.
- Kumar, A., 2016. Stability testing of herbal products. *J. Chem. Pharmaceut. Res.* 7, 511–514.
- Li, L.L., Cui, Y., Guo, X.H., Ma, K., Tian, P., Feng, J., Wang, J.M., 2019. Pharmacokinetics and tissue distribution of gingerols and shogaols from ginger (*Zingiber officinale* rosc.) in rats by UPLC–Q-Exactive–HRMS. *Molecules* 24, 1–12.
- Madruca, M.S., De Albuquerque, F.S.M., Silva, I.R.A., Do Amaral, D.S., Magnani, M., Neto, V.Q., 2014. Chemical, morphological and functional properties of Brazilian jackfruit (*Artocarpus heterophyllus* L.) seeds starch. *Food Chem.* 143, 440–445.
- Olalere, O.A., Abdurahman, H., Bin, R., Yunus, M., Alara, O.R., 2018a. Data Article on Elemental and Metabolomic-Based Alkaloidal Composition in Black Pepper Oleoresin Using a Positive ESI-Mode LC-QToF and ICP-Mass Spectroscopy.
- Olalere, O.A., Abdurahman, H.N., Gan, C.Y., 2019. Microwave-enhanced extraction and mass spectrometry fingerprints of polyphenolic constituents in *Sesamum indicum* leaves. *Ind. Crop. Prod.* 131, 151–159.
- Olalere, O.A., Abdurahman, N.H., Alara, O.R., Habeeb, O.A., 2017. Parametric optimization of microwave reflux extraction of spice oleoresin from white pepper (*Piper nigrum*). *J. Anal. Sci. Technol.* 8, 8.
- Olalere, O.A., Abdurahman, N.H., Yunus, R., bin, M., Alara, O.R., Gan, C.Y., 2018b. Synergistic intermittent heating and energy intensification of scale-up parameters in an optimized microwave extraction process. *Chem. Eng. Process. - Process Intensif.* 132, 160–168.
- Paunović, D.Đ., Mitić, S.S., Kostić, D. a, Mitić, M.N., 2014. Kinetics and Thermodynamics of the Solid-Liquid Extraction Process of Total Polyphenols from Barley, pp. 58–63, 3.
- Ranasinghe, R.A.S.N., Maduwanthi, S.D.T., Marapana, R.A.U.J., 2019. Nutritional and health benefits of jackfruit (*Artocarpus heterophyllus* lam.): a review. *Int. J. Food Sci.* 1–13, 2019.
- Senwal, R.B., Senwal, D.K., Combrinck, S., Viljoen, A.M., 2015. Gingerols and shogaols: important nutraceutical principles from ginger. *Phytochemistry* 117, 554–568.
- Silva, D.F., Olímpia, M., Rezende, O., 2016. Microwave-assisted Extraction of Phenolic Compounds from *Canavalia Ensiformis* Leaves : Preparation and Evaluation of Prospective Bioherbicide on Control of Soybean Weeds 106–111.
- Sur, B., Kang, S., Kim, M., Oh, S., 2019. Inhibition of carrageenan/kaolin-induced arthritis in rats and of inflammatory cytokine expressions in human IL-1 $\beta$ -stimulated fibroblast-like synoviocytes by a benzylideneacetophenone derivative. *Inflammation* 42, 928–936.
- Surat, M.a., Jauhari, S., Desak, K.R., 2012. A brief review : microwave assisted organic reaction. *Appl. Sci. Res.* 4, 645–661.
- Theophanides, T., 2012. Introduction to infrared spectroscopy. In: *Infrared Spectroscopy - Materials Science, Engineering and Technology*, pp. 1–10.
- Veggi, P.C., Martinez, J., Meireles, M.A.A., 2013. Microwave-assisted extraction for bioactive compounds. *Theory and Practice Springer Science & Business Media* 4.
- Wang, L., Wang, P., Wang, D., Tao, M., Xu, W., Olatunji, O.J., 2020. Anti-inflammatory activities of kukoamine A from the root bark of *Lycium chinense* miller. *Nat. Prod. Commun.* 15.
- Wang, S., Zhang, Q., Zhang, Yuxin, Shen, C., Wang, Z., Wu, Q., Zhang, Yanling, Li, S., Qiao, Y., 2016. Agrimol B suppresses adipogenesis through modulation of SIRT1-PPAR gamma signal pathway. *Biochem. Biophys. Res. Commun.* 477, 454–460.
- Xiao, L., Huang, Y., Wang, Y., Xu, J., He, X., 2020. Anti-neuroinflammatory benzofurans and lignans from *Praxelis clematidea*. *Fitoterapia* 140, 104440.
- Xu, M.Y., Lee, D.H., Joo, E.J., Son, K.H., Kim, Y.S., 2013. Akebia saponin PA induces autophagic and apoptotic cell death in AGS human gastric cancer cells. *Food Chem. Toxicol.* 59, 703–708.
- Yang, D., Cheng, Z.Q., Yang, L., Hou, B., Yang, J., Li, X.N., Zi, C.T., Dong, F.W., Liu, Z.H., Zhou, J., Ding, Z.T., Hu, J.M., 2018. Seco-dendrobine-type Alkaloids and bioactive phenolics from *dendrobium findlayanum*. *J. Nat. Prod.* 81, 227–235.
- Yuan, Y., Macquarrie, D., 2015. Microwave assisted extraction of sulfated polysaccharides ( fucoidan ) from *Ascophyllum nodosum* and its antioxidant activity. *Carbohydr. Polym.* 129, 101–107.
- Zhang, Y., Zhu, K., He, S., Tan, L., Kong, X., 2016. Characterizations of high purity starches isolated from five different jackfruit cultivars. *Food Hydrocolloids* 52, 785–794.
- Zhang, Yanjun, Zhang, Yutong, Xu, F., Li, S., Tan, L., 2018. Food Hydrocolloids Structural characterization of starches from Chinese jackfruit seeds ( *Artocarpus heterophyllus* Lam ). *Food Hydrocolloids* 80, 141–148.
- Zhang, Yutong, Zhang, Yanjun, Li, B., Wang, X., Xu, F., Zhu, K., Tan, L., Dong, W., Chu, Z., Li, S., 2019. In vitro hydrolysis and estimated glycemic index of jackfruit seed starch prepared by improved extrusion cooking technology. *Int. J. Biol. Macromol.* 121, 1109–1117.